Research Paper

PAIN 00 (2024) 1–17

PAIN®

OPEN

Reorganization of lateral habenula neuronal connectivity underlies pain-related impairment in spatial memory encoding

Helder Cardoso-Cruz[a,b,c,*], Clara Monteiro[a,b,c], Vasco Galhardo[a,b,c]

Abstract

Dysfunctional hyperactivity of the lateral habenula nucleus (LHb) has emerged as a critical marker for pain-related mood impairments. Acting as a central hub, the LHb filters and disseminates pertinent information to other brain structures during learning. However, it is not well understood how intra-LHb activity is altered during cognitive demand under neuropathic pain conditions. To address this gap, we implanted an optrode structure to record neuronal activity in adult male CD (rat strain without definition) rats during the execution of a delayed nonmatch-to-sample (DNMS) spatial working memory (WM) task. We selectively modulated intra-LHb network activity by optogenetically inhibiting local LHb CaMKIIα (calcium calmodulin-dependent protein kinase II alpha)-expressing neurons during the delay phase of the DNMS task. Behavioral assessments were conducted using a persistent rodent model of neuropathic pain—spared nerve injury. Our results showed that the induction of neuropathic pain disrupted WM encoding accuracy and intra-LHb functional neuronal connectivity. This disruption was reversed by optogenetic inhibition of LHb CaMKIIα-expressing neurons, which also produced antinociceptive effects. Together, our findings provide insight into how intra-LHb networks reorganize information to support different task contexts, suggesting that the abnormal pain-related intra-LHb dynamic segregation of information may contribute to poor cognitive accuracy in male rodents during pain experiences.

Keywords: Lateral habenula, Working memory, Neuropathic pain, Intra-connectivity, Optogenetic glutamatergic neurons inhibition, In vivo extracellular multielectrode recordings, Partial directed coherence, Spared nerve injury

1. Introduction

Several studies have suggested that the impact of pain on the brain could be cumulative over time, and its severity is strictly linked to the probability of developing mood disorders and cognitive impairments.[17,32,37,57,61,67] Considering that a primary predictor of susceptibility to mood disorders involves the emergence of negative emotional states, this may partially account for the elevated prevalence of conditions like learning and memory impairments among patients with chronic pain.[17,24,54,58,61,68]

The past decade has witnessed a significant increase in interest regarding the role of the lateral habenula (LHb) in regulating the ability to make appropriate decisions that result in a balanced outcome in response to changing contexts.[55,56] The LHb acts as a central hub that filters and transmits relevant information between the forebrain and midbrain regions[39,40,50,62] and is involved in regulating both innate and learned behaviors playing an essential role in shaping responses based on the value of choices.[6,7,52,56,72]

The LHb also has been shown to play a crucial role in regulating the experience of pain.[45] This brain area exhibits a close functional and morphological interplay with other brain centers involved in pain and emotional response processing.[11,70] Imaging studies have shown that the habenular complex is activated or displays abnormal activity regimes in patients with chronic pain, leading to functional changes that might impact high-level cognitive functions.[11,64] Moreover, high-frequency deep brain stimulation has been employed to alleviate depressive symptoms in patients,[66] and lesions in the LHb can reverse depression-like behaviors in rodents.[44,80] Nevertheless, the underlying mechanisms by which pain affects the LHb and its role in impairing spatial working memory (WM) remains unclear.

Previous studies have reported decreased metabolic activity in the LHb in rats with impaired memory.[42] Activation of LHb GABAergic receptors has been shown to impair spatial WM.[30] Electrical stimulation of the LHb impairs cognitive performance in rats.[42,72] Furthermore, pharmacological inactivation of the LHb induces hippocampus-dependent memory deficits.[51] The LHb interacts with the hippocampal formation, participating in hippocampal-dependent spatial information processing,[30] as evidenced by its synchronism with hippocampal theta oscillations.[2] On the other

Sponsorships or competing interests that may be relevant to content are disclosed at the end of this article.

[a] Instituto de Investigação e Inovação em Saúde (i3S), Pain Neurobiology Research Group, Universidade do Porto, Porto, Portugal, [b] Instituto de Biologia Molecular e Celular (IBMC), Universidade do Porto, Porto, Portugal, [c] Faculdade de Medicina (FMUP), Departamento de Biomedicina—Unidade de Biologia Experimental, Universidade do Porto, Porto, Portugal

**Corresponding author. Address: Faculdade de Medicina da Universidade do Porto, Departamento de Biomedicina, Unidade de Biologia Experimental, Piso 4, Rua Doutor Plácido da Costa, 4200-450 Porto, Portugal. Tel.: +351 225 513 600; fax: +351 225 513 601. E-mail address: hcruz@med.up.pt (H. Cardoso-Cruz).*

Supplemental digital content is available for this article. Direct URL citations appear in the printed text and are provided in the HTML and PDF versions of this article on the journal's Web site (www.painjournalonline.com).

http://dx.doi.org/10.1097/j.pain.0000000000003493

hand, studies have shown that lesions of the LHb improve WM in hemiparkinsonian rats.[25] In addition, pharmacological modulation of LHb serotonin receptors has been demonstrated to improve WM in Parkinson's rats,[31] and the activity of nicotinic receptors in the LHb plays also a significant role in spatial memory function.[65] A recent study from our laboratory has also observed that selective optogenetic inhibition of LHb glutamatergic neurons projecting into the ventral tegmental area (VTA) enhances WM in inflammatory pain rats.[3] These studies suggest that LHb dysfunction is an important factor in the impairment of memory.

In this study, we explored the reorganization of the internal LHb network in a rodent model of neuropathic pain and its association with impaired memory. Our hypothesis is that neuropathic pain induces plastic changes in the LHb, resulting in altered LHb activity and subsequent spatial memory deficits.

2. Material and methods

2.1. Rodent model and ethical statement

2.1.1. Experimental rodent model

Experiments were conducted on adult male Sprague-Dawley rats weighting 275 to 325 g at the beginning of the experiment (obtained from Charles River Laboratories, Saint Germain Neulles, France). The rats were housed under standard laboratory conditions in an individual ventilated cage unit (model IVC Smart flow; Tecniplast, Buguggiate, Varese, Italy), with a simulated 12-hour light/dark cycle (lights on from 7:30 to 19:30), maintained at a constant temperature of 22 ± 2°C and a relative humidity of 50 ± 5%. Before behavior and stereotaxic surgery protocols, the rats were kept in collective cages (4 per cage; model GR1800 Double Decker, Tecniplast). After optrode implantation or LHb lesion, the rats were housed individually. Training and recording sessions were always conducted during the light cycle at approximately the same time each day. All rats were food-deprived to 90% to 95% of their ad libitum free-feeding body weights while having unrestricted access to water throughout the behavioral experiments. The rats were habituated to being handled by the experimenters before the start of any experimental procedures.

2.1.2. Ethical statement

All behavioral and electrophysiological procedures were conducted in accordance with the guidelines outlined in the European Union directive 2010/63/CE, and Research and Ethical Issues of the International Association for the Study of Pain.[81] The experimental protocols received approval from both the local Ethical Committee of the Faculty of Medicine of the University of Porto (ORBEA; Porto, Portugal) (project number 82) and the national Direção Geral de Alimentação e Veterinária board (DGAV; Lisbon, Portugal) (project reference 008335 of 2019/04/11). Throughout manipulations involving the rats, at least 1 experimenter certified under FELASA category C was present. The ARRIVE guidelines were followed. Every effort was undertaken to adhere to the 3R's recommendations for animal experimentation, minimizing animal distress and utilizing the minimum number of animals necessary.

2.2. Surgical procedures

2.2.1. Virus injection and optrode implantation

For the surgical interventions, the rats were anesthetized with an intraperitoneal (I. P.) injection of a medetomidine and ketamine mixture (at doses of 0.5 and 75 mg/kg, respectively). The depth of anesthesia and muscular paralysis were regularly assessed by testing the corneal blink, hindpaw withdrawal, and tail-pinch reflexes. Anesthesia was maintained through small additional ketamine injections (one-third of the initial dosage, IP). Following induction of anesthesia, each rat received 1 mL of 2% wt/vol sucrose in 0.9% wt/vol NaCl, subcutaneous (S. C.) every hour throughout the surgery. This step is particularly important to prevent dehydration during long surgical procedures. Core body temperature was maintained at 37°C using a thermal blanket. Before positioning the rats in the stereotaxic frame, their fur was trimmed, and ocular gel (Lubrithal, Dechra, United Kingdom) was applied to protect their eyes. The rats were secured in a stereotaxic frame using ear bars, and the skull was exposed and cleaned using hydrogen peroxide. A 3 mm^2 hole was drilled into the skull to serve as the entry point for the optrode. Up to 5 screws were fixed into the skull to hold the optrode structure in place. A silver wire (with a diameter of 200 μm) was attached to the skull-fixed screws with silver paste, serving as a grounding reference. The coordinates for targeting the LHb were determined using the stereotaxic atlas[60]: 3.2 to 3.6 mm posterior to bregma, 0.7 to 0.9 mm lateral to midline, and 4.8 to 4.9 mm depth from the dura mater. Before the optrode implantation, 1 μL of viral particles (see details below) was injected into the LHb at a rate of 0.1 μL/minute, using a 5-μL microsyringe (Model 7105 KH—type 2; Hamilton, Reno, NV). The microsyringe was left in place for an additional 10 minutes to facilitate the diffusion of the virus before being gradually withdrawn. Adeno-associated viruses (AAVs) of serotype 1, encoding the halorhodopsin (eNpHR3.0 variant) or control, were acquired from Addgene (Cat. No. 26971). Viral titers were 6.0×10^{12} particles/mL for AAV1-CaMKIIα-eNpHR3.0-eYFP and 4.0×10^{12} particles/mL for AAV1-CaMKIIα-mCherry (Cat. No. 114469). The utilization of a calcium calmodulin-dependent protein kinase II alpha (CaMKIIa)-promoter enables transgene expression primarily in excitatory neurons.[29] The viruses were stored in a −80°C freezer until the day of injection. Subsequently, the optrode comprising an optical fiber affixed to an 8-channel multielectrode bundle (constructed with Tungsten Formvar-coated filaments of 35-μm diameter, possessing an impedance range of 0.7-1.2 MΩ; obtained from California Fine Wire Company, Grover, CA), was positioned into a hydraulic micropositioner (FHC Instruments Inc., Bowdoin, ME) and then slowly driven into the LHb at a rate of 100 μm/minute. Given the known asymmetries of the habenula[10] and the differential impact of left- or right-side neuropathy on cognitive function in rodents,[43] we opted to perform unilateral interventions counterbalanced between brain hemispheres across rats (Appendix B: supplementary data—Table T1, http://links.lww.com/PAIN/C185).

Unilateral interventions were chosen to minimize potential confounding effects and isolate the functional contributions of the LHb more effectively. This approach allows for the assessment of lateralized effects on behavior while avoiding complete disruption of bilateral neural pathways. In addition, unilateral interventions can provide insights into compensatory mechanisms in the unaffected hemisphere, helping to clarify the specific role of the LHb in behavior and cognitive functions without the complications introduced by bilateral lesions. The optrode was implanted contralateral to the peripheral lesion and secured to the skull using dental acrylic cement. After the surgical procedures, an analgesic (ketoprofen, 5 mg/kg) and an antibiotic (enrofloxacin, 5 mg/kg) diluted 1/5 in saline were administered subcutaneously every 24 hours for 5 to 7 days to improve postoperative recovery. Their overall health condition was monitored daily.

2.2.2. Neuropathic pain model

Immediately after optrode implantation, each rat underwent the spared nerve injury (SNI) rodent model of neuropathic pain (ahead

referred to as the SNI group)[23] or a control intervention involving the same extent of skin incision and muscle dissection (ahead referred to as the sham group). Both surgical interventions were carried out on the contralateral hindpaw to the side of optrode implantation. The sensory threshold for noxious mechanical stimulation was assessed using von Frey filaments (Somedic Inc., Sösdala, Sweden) employing the Dixon up-down method with incremental logarithmically stiffness filaments (7, 8, 11, 14, 18, 23, 38, 49, 53, and 90 g/mm^2). Rats were placed individually in a square chamber positioned over a mesh table, and they were allowed to acclimate for a period of 20 to 30 minutes. Von Frey filaments were applied to the lateral one-third of the hindpaw, targeting the distribution of the sural nerve. In the case of optogenetic protocols, these measurements were performed in independent sessions, with and without optogenetic light stimulation (10-second continuous pulse/trial; stimulation physical parameters below).

2.3. Experimental design and behavioral procedures

2.3.1. Spatial working memory task

In this study, we investigated the effect of optogenetic inhibition of LHb CaMKIIα-expressing neurons on WM performance. To achieve this, we employed a delayed nonmatch-to-sample (DNMS) task, which has been previously described[16] (**Fig. 1A**). Each trial consisted of a sample phase (memory formation) during which 1 of the levers was exposed until the rat pressed it within a time limit of 20 seconds. After the lever press, a delay phase was initiated. Performance was assessed using 3 delay-phase challenges: 1 second (for learning curve), and 5 and 10 seconds (for probe sessions). Following the delay phase, a nonmatch phase (memory retrieval) began, during which both retractable levers were exposed until the rat pressed one within a time limit of 30 seconds. A trial was rewarded with a food pellet when the rat pressed the opposite lever (correct trials), which had been presented during the sample phase. A trial was considered wrong and nonrewarded when the rat pressed the same lever presented during the sample phase. If the rat failed to respond to the lever within the imposed time limit, the trial was classified as an omission. Trials were separated by a 15-second interval. Before initiating the probe sessions, each rat was placed in the testing arena and connected to an electrophysiological wireless headstage transmitter (model W16; Triangle Biosystems, Durham, NC) and an optical patch cable that was connected to a dual LED source commutator (PlexonBright; Plexon Inc., Dallas, TX). To acclimate the rats to the experimental setup conditions, a habituation protocol was applied using a DNMS delay-phase challenge of 1 second (3 consecutive days, 50 trials/session). Each probe session consisted of 100 trials. A timeline diagram of the experimental design is illustrated in **Figure 1B**. The feeder and retractable levers were fully automated and controlled using the OpenControl software customized for this task.[1] The reward pellets used throughout the experiments were 45 mg sucrose dustless precision reward pellets (Cat No. F0023; Bioserv, Frenchtown, NJ). All behavioral experiments were conducted during the light phase in a light-attenuated room. To minimize possible bias, especially related to the testing group, rats from different experimental groups were tested alternately. The experimenter was blinded to the experimental group treatments.

2.3.2. Optogenetics and light neuromodulation

Neurophysiological recordings commenced 3 weeks after viral injection and optrode implantation to ensure sufficient tissue expression and stability of the SNI model. During behavioral testing, external patch cords (200 μm diameter, 0.66 NA, Plexon Inc.) were connected to the implanted optical fiber using sleeves. The optical fiber was placed unilaterally in the LHb, as previously described. A commutator with a 620 nm wavelength LED light source was used for light delivery (PlexonBright, Plexon Inc.). The inhibition experiments employed 5 to 6 mW of light intensity (158-189.6 mW/mm^2 at the fiber tip), and continuous irradiance at the fiber tip was verified before implantation using a light power meter (model PM160; ThorLabs, Munich, Germany). To prevent light scattering from acting as a cue for rats, the interface between the optical patch cord zirconia ferrule and the implanted optical fiber was shielded with black adhesive tape. Light stimulation was delivered during the entire delay-phase period of the DNMS task. This time window in WM-dependent tasks is particularly important for actively holding goal-related information and preparing forthcoming actions.[21,63]

2.3.3. In vivo extracellular electrophysiological recordings

Neurophysiological signals were recorded from the LHb during the performance of the DNMS task. The 8-channel multielectrode bundle was linked to a wireless high-frequency headstage transmitter (W16; Triangle Biosystems), which transmitted continuous analog signals to a 16-channel Multichannel Acquisition Processor system (16-MAP; Plexon Inc.). The neural signals were preamplified (10,000-20,000X) and digitized with a frequency of sampling of 40 kHz. Voltage-time threshold windows were employed to identify single-unit waveforms. These waveforms were sorted online through SortClient 2.6 software (Plexon Inc.) and later verified offline using a combination of automatic and manual sorting techniques (Offline Sorter 2.8; Plexon Inc.) based on the cumulative criteria described in detail elsewhere.[15] A maximum of 3 neuronal action potentials were recorded per channel. Only units that exhibited stable spike amplitudes and consistent waveforms across recording sessions were considered for inclusion in this study. Subsequently, this data was processed offline using NeuroExplorer 4 software (NEX 4, Plexon Inc.) and then exported to MatLab (R2023a, MathWorks, Natick, MA) for further analysis through custom routines.

2.3.4. Anatomical and histological validation

After the completion of the last electrophysiological recording session, rats were deeply anesthetized using pentobarbital sodium (175 mg/kg, i. p.) and transcardially perfused with 0.01 M phosphate buffer in saline (pH = 7.2) followed by 4% paraformaldehyde. Following the perfusion, the brains were carefully extracted and underwent postfixation in a 4% paraformaldehyde for a duration of 4 hours. Following postfixation, the brains were immersed in a 30% (wt/vol) sucrose solution for preservation purposes. Once appropriately saturated, the brains were frozen and sliced into 40-μm coronal sections. These coronal brain sections were mounted on gel-coated laminas and counterstained with thionine to aid visualization of tissue damage extension or the optrode tracks under a light microscope. To verify opsin expression, the transfected coronal slices were incubated in DAPI (2 mg/mL in glycerol-mounting media) for cell nucleus staining. The stained sections were observed using a Zeiss Z1 Apotome microscope. To ascertain their final location, a rat brain atlas[60] was used. The comparison to the reference atlas was assessed by an experimenter blinded to the experimental contingencies. Only rats with correctly located implanted optrodes and successful viral expression were included in the

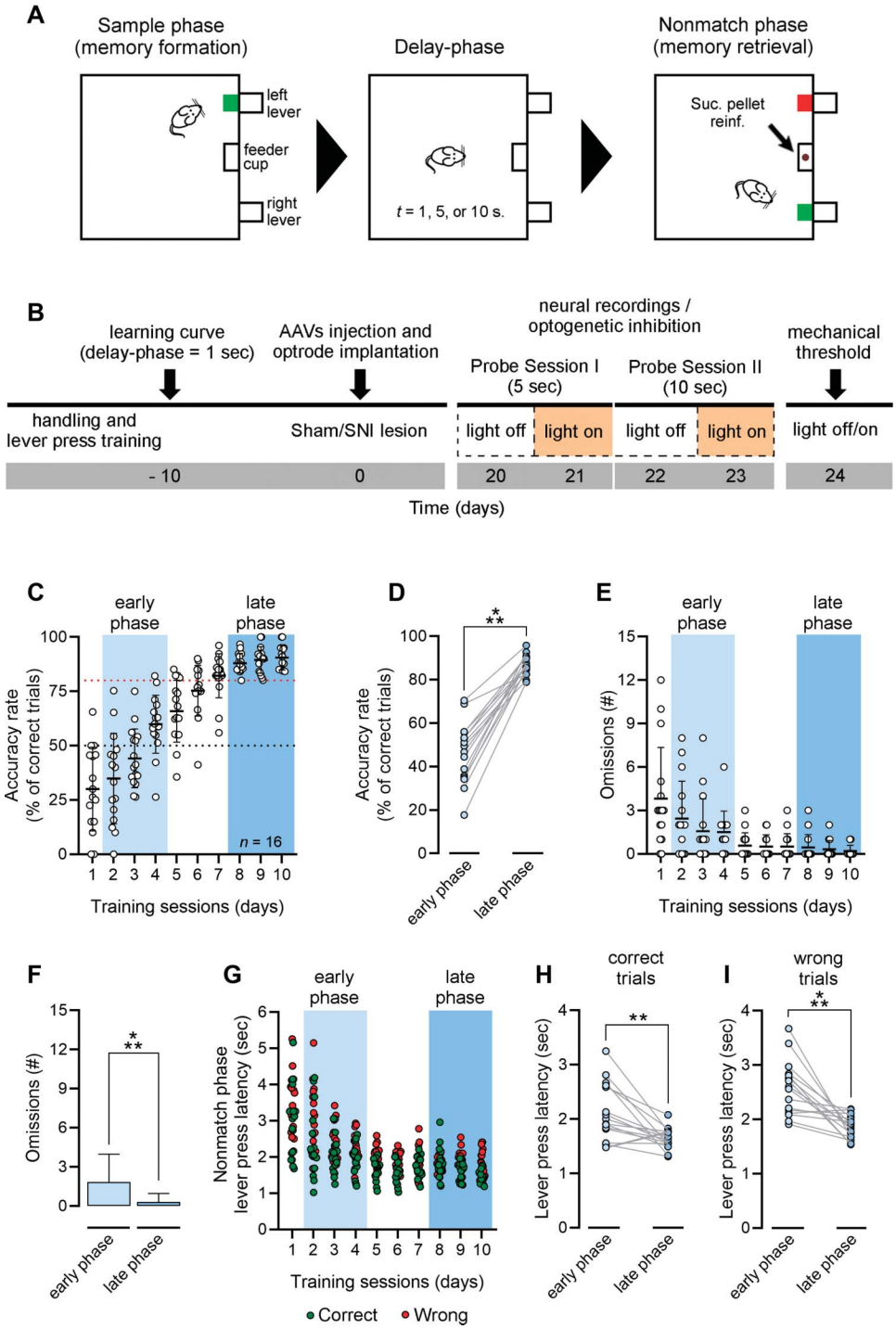

FIGURE 1. Delayed nonmatch-to-sample working memory task, experimental timeline, and learning curve. (A) Diagram of delayed nonmatch-to-sample (DNMS) working memory task used in this study. In brief, each trial began with a single retractable lever (green square) being exposed (sample phase, memory formation). When the rat pressed the lever, it retracted and the delay phase was initiated. Three DNMS delay-phase challenges were used: 1 second (learning phase), and 5 and 10 seconds (probe sessions). At the end of this phase, both retractable levers were exposed (nonmatch phase, memory retrieval), and the rat should press the opposite lever during the sample phase to obtain a reward pellet. (B) Timeline of the experimental protocol. After the learning curve, each rat was implanted with an optrode in the LHb and subjected to a contralateral sham or spared nerve injury model (SNI) lesion. After the postoperative recovery, rats were subjected to 2 probe sessions in each respective DNMS task delay-phase challenge, without and with photoinhibition. (C) Distribution of correct responses for all rats across 10 daily sessions of the learning curve using a delay-phase challenge of 1 second. Shaded regions denote the range of days from which the early and late phase learning curve analyses were performed. (D) The percentage of correct trials for all rats increased significantly from the early phase (light blue) to the late phase (blue) in learning. (E) Distribution of omissions for all rats across 10 daily sessions. (F) The number of omissions performed for all rats decreased significantly from the early phase (light blue) to the late phase (blue) in learning. (G) Distribution of the averaged nonmatch lever press response latency of correct and wrong trials for all rats across 10 daily sessions. (H) Response latency of correct (central panel) and (I) wrong (right panel) trials decreased significantly from the early phase (light blue) to the late phase (blue) in learning. Comparisons of learning phases were performed using a nonparametric Wilcoxon matched-pairs signed rank test (2-tailed, $P < 0.05$). Rats, n =16. Significant results are indicated by ** when $P < 0.01$ and *** when $P < 0.001$. LHb, lateral habenula.

data analysis. The locations of the placement of the optrodes were plotted onto standard diagrams for further reference and analysis.

2.4. Offline data analysis, representations, and statistics

2.4.1. Offline data analysis and representations

To evaluate the functional impact of light stimulation on the recorded LHb units, we compared the mean baseline activity of each unit before, during, and after a 5-second light-on period of stimulation. Subsequently, we categorized these units based on their firing activity, classifying them as having increased, unchanged, or decreased activity. We employed custom MatLab scripts to define behavioral response time windows based on trial outcomes (correct vs wrong trials), the sample phase, the delay phase, and the nonmatch phase. For the analysis of neuronal activity in relation to behavioral responses, we selected behavioral sessions with a minimum of 5% wrong trials. To depict neuronal activity correlations based on their average responses per probe session, we initially computed the perievent time histogram (PETH) for each neuron using a time window corresponding to the duration of the DNMS delay phase (5 or 10 seconds). For neuronal correlations related to correct and wrong responses, we used a time window of −2 to +2 seconds, centered around the nonmatch phase lever press. Because most of the examined parameters are affected by low-firing rates, neurons with firing rates <0.1 Hz were not analyzed. Furthermore, to ensure that the same unit was being recorded across repeated sessions, only units that exhibited stable spike amplitudes and consistent waveforms both within and between recording sessions were included in this study. Next, we computed the average activity of all recorded units per behavioral contingency to assess their response distribution. Perievent time histograms were generated with a bin resolution of 50 milliseconds and further smoothed using the native MatLab function "*interp1*" applying a 3° smoothing technique. To determine whether the independent behavioral neuronal activity traces during different behavioral conditions exhibited distinct distribution functions, we employed the 2-sample Kolmogorov-Smirnov goodness-of-fit hypothesis test (*kstest2*, $P < 0.05$) applying the native MatLab function "*kstest2*." For the recorded activity during mechanical sensitivity testing, we calculated the average PETH of LHb activity for the final selected response filament, centering the calculation on the response timestamp. The resultant data were presented as the average of positive responses across 10 trials (see details in section 2.2.3.). Next, neuronal activity heatmaps were computed with a bin resolution of 250 milliseconds and horizontally smoothed (3°). The vertical values on the right side of each panel corresponded to the pressure evoked by the final von Frey hair filament selected. To compare the average activity distributions under different experimental contingencies, we employed a time window ranging from −1 second to +3 seconds postresponse to the von Frey filament and used the 2-sample Kolmogorov-Smirnov test (*kstest2*, $P < 0.05$). To assess the neuronal paired connectivity within the intra-LHb network during rewarded and nonrewarded trials, we applied the partial directed coherence (PDC) statistical method, which has been previously described in detail.[5] PDC is a technique for analyzing multivariate processes that involve Granger causality to reveal domains of direct influence and assess interactions between structures and their directionality. The PDC value ranges from 0 to 1, in which PDC = 0 indicates the absence of functional connectivity between structures, while PDC = 1 indicates strong functional connectivity. We calculated the intra-LHb paired PDC activity trial-by-trial during 10-second delay-phase challenge sessions, using a 4-second time window centered on the nonmatch phase lever press response. We chose to use this contingency because it includes a better balance of rewarded vs nonrewarded trials. The average PDC activity was then depicted separately for correct and wrong trials. Cross-paired activity of the recorded units was represented using histograms with an interval resolution of 0.05.

2.4.2. Statistical analysis

Statistical analysis was conducted using GraphPad Prism version 9 (GraphPad Software, Inc., La Jolla, CA) and native MatLab functions (MathWorks). All values were tested for normality using the Kolmogorov-Smirnov (*k*stest) test (with Dallal-Wilkinson-Lilliefor for correct *P*-value). Parametric tests were used when *k*stest > 0.05. For single comparisons, we used a nonparametric Wilcoxon marched-pairs signed rank test (*W*) (2-tailed) for paired samples; otherwise for multiple comparisons, we used a nonparametric Kruskal-Wallis test (*KW*) or a nonparametric Friedman test (*F*) (for repeated measures) followed by the Dunn post hoc test. Single data points are always plotted. For behavioral experiments, the sample size was preestimated based on previously published research, pilot experiments conducted in the laboratory, and in-house expertise. Rats were randomly assigned to experimental groups, and each rat represented an analytical unit. We stated the replication factor for each experiment. All effects presented as statistically significant exceeded an α-threshold of 0.05, and all independence tests were 2-tailed. Data in the text are presented as mean ± standard deviation (SD).

3. Results

3.1. Learning phase and delay nonmatch-to-sample working memory task

We used a DNMS paradigm to examine the impact of neuropathic pain on the intra-LHb networks during cognitive demand (**Fig. 1A**). The experimental setup and timeline for the behavioral and neuromodulation protocols are illustrated in **Figure 1B**. In brief, rats were trained using a delay-phase challenge of 1 second (learning phase). All rats included in this study (n = 16) reached the inclusion criterion after completing 10 daily training sessions (**Fig. 1C**). As commonly observed in goal-directed tasks, there was a phase of rapid improvement followed by a phase of stabilized learning, representing early (days 2-4) and late (days 8-10) phases of learning. The percentage of correct trials increased from early to late phase of learning (**Fig. 1D**; Wilcoxon test $P < 0.001$), leading to a reduction in the number of omissions over time (**Figs. 1E and F**; $P < 0.001$). Rats also exhibited a global decrease in the mean nonmatch lever press latency from early to late phase of learning (**Fig. 1G**), across correct (**Fig. 1H**; $P = 0.0027$) and wrong trials (**Fig. 1I**, $P < 0.001$).

3.2. Optogenetic inhibition of lateral habenula CaMKIIα-expressing neurons

We used an in vivo approach to study the role of LHb CaMKIIα-expressing neurons in pain-related WM deficits. **Figures 2A and B** show a schematic illustration of the viral injection protocol used in the LHb and the experimental setup used to record neuronal activity. Three weeks after AAV1-CaMKIIa-eNpHR3.0-

mCherry injection into the LHb, a robust opsin expression was observed in LHb neurons (**Fig. 2C**). The correct targeting of optrode implantation in the LHb was verified after the behavioral studies by brain cryosectioning. A representative example of optrode location is given in **Figure 2D**. From an initial pool of 16 rats, 5 rats were excluded due to incorrect optrode final location and/or viral expression. We recorded a total of 138 neurons from eNpHR3.0-expressing rats in the LHb (sham group, n = 61; and SNI group, n = 77). To test the functional efficiency of viral transfection and light stimulation, we compared the mean firing activity before, during, and after a 5-second light-on vs light-off protocol (**Fig. 2E**). Optical activation of eNpHR3.0 (620 nm orange led; 5 seconds constant light at 5-6 mW) lead to a general decrease in the LHb neuronal firing rate in sham rats (**Fig. 2E**—left panel; Friedman test $F = 13.41$, $P = 0.0012$, post hoc Dunn test: before vs during stimulus $P = 0.0012$, and during vs after stimulus $P = 0.0296$) and in SNI rats (**Fig. 2E**—right panel; $F = 70.13$, $P < 0.0001$, post hoc Dunn test: before vs during stimulus $P < 0.0001$, and during vs after stimulus $P < 0.0001$). The percentage of recorded units with altered activity is shown in **Figure 2F**.

3.3. Selective inhibition of lateral habenula neurons improved working memory performance during higher complexity challenges

We next examined the behavioral effect of optogenetic inhibition of LHb CaMKIIα-expressing neurons during the performance of the DNMS task with 2 different delay-phase complexity challenges (**Fig. 3A**). In probe sessions with 5 seconds of delay-phase challenge, no significant effects were observed in the accuracy rate between experimental groups or light modulation protocols (*KW* = 1.06, *P* = 0.7869 [n.s.]; **Fig. 3B**—left panel). For 10 seconds of delay-phase challenge, statistical analysis showed a significant effect between experimental groups across light treatments (*KW* = 9.04, *P* = 0.0288; **Fig. 3B**—right panel); moreover, post hoc test showed that SNI-treated rats increased their performance when LHb CaMKIIα-expressing neurons were inhibited (SNI: light-off vs light-on protocol, $P < 0.05$, Dunn test). Interestingly, these changes observed in the accuracy rate did not lead to changes in the number of omissions (5 seconds: *KW* = 6.40, *P* = 0.0936 [n.s.], **Fig. 3C**—left panel; and 10 seconds: *KW* = 4.64, *P* = 0.1999 [n.s.], **Fig. 3C**—right panel). Another important observation was the nonmatch lever press response latency exhibited by both experimental groups. In the case of correct trials, no significant differences were observed in all behavioral contingencies (5 seconds: *KW* = 1.33, *P* = 0.7222, and 10 seconds: *KW* = 6.03, *P* = 0.1104; **Fig. 3D**—top panels respectively). In the case of wrong trials, both behavioral contingencies revealed significant effects between experimental groups and light neuromodulation protocols (5 seconds: *KW* = 8.62, *P* = 0.0347; **Fig. 3D**—bottom left panel; and 10 seconds: *KW* = 13.06, *P* = 0.0045). Furthermore, our data revealed that during wrong trials the sham-treated rats spent more time to select the lever in either delay-phase challenges when compared with SNI rats (5 and 10 seconds: light-off sham vs SNI, both $P < 0.05$; **Fig. 3D**—bottom panels). Furthermore, our results suggest that the time needed to make a response may have an impact on executing a correct response, as evidenced by the fact that sham-treated rats decreased their nonmatch lever press response latency during inhibition of LHb CaMKIIα-expressing neurons (10 seconds: sham, light off vs light on, $P < 0.05$).

3.4. Changes in neuropathic pain threshold in spared nerve injury rats during optogenetic inhibition of lateral habenula CaMKIIα-expressing neurons

To further evaluate the role of LHb CaMKIIα-expressing neurons in pain response, we examined the neuropathic pain threshold 24 days after peripheral nerve lesion using von Frey filaments during optogenetic neuromodulation. The neuropathic pain threshold in the SNI-treated rats had a significant increase during photoinhibition protocols compared with the absence of light neuromodulation (*KW* = 13.49, *P* = 0.0037; SNI group: light-off vs on, $P < 0.05$; light-off: sham group vs SNI group, $P < 0.01$, Dunn post hoc test; **Fig. 3E**). This result suggests that inhibiting LHb CaMKIIα-expressing neurons may improve hyperalgesia in SNI-treated rats without sensitizing sham-treated rats. Next, we evaluated the normalized mean firing activity recorded per rat during mechanical stimulation with the filament selected (**Fig. 3F**). Without light stimulation, heatmaps revealed that SNI-treated rats showed a clear higher neuronal firing rate activity when compared with control animals (**Fig. 3F**—top left panels), resulting also in a different neuronal activity distribution (light off: sham vs SNI, *kstest2* = 0.8788, $P < 0.0001$; **Fig. 3F**—top right panel). By contrast, during light stimulation protocol, both experimental groups revealed a similar pattern of response (**Fig. 3F**—bottom left panels), resulting also in similar levels of neuronal activity (light on: *kstest2* = 0.1212, *P* = 0.9570 [n.s.]; **Fig. 3F**—bottom right panel). Supplementary data on the impact of optogenetic stimulation in rats transfected with the control virus AAV1-CaMKIIα-mCherry on behavior and LHb activity are provided in supplementary Fig. S4 (Appendix A, http://links.lww.com/PAIN/C184).

3.5. Lateral habenula neurons exhibited dynamic firing activity throughout the delay phase of the delayed nonmatch-to-sample task, which precedes the lever selection

The delay phase in WM tasks is critical for maintaining task-relevant information and preparing accurate decision responses, with neural activity in subcortical regions like the LHb playing key roles.[25,50] We assessed the effectiveness of light neuromodulation on the average firing activity during the DNMS delay-phase cognitive demand (**Fig. 4A**), with data segmented for correct and wrong trials. A 2-sample Kolmogorov-Smirnov test (*kstest2*, $P < 0.05$) was used to compare differences in firing distributions. Across most contingencies, each group exhibited distinct activity profiles under cognitive demand during light stimulation protocols. The most prominent differences were observed in trials associated with wrong responses. In correct trials (**Fig. 4B**), there were no significant differences between experimental groups and light delivery protocols during the delay phase for both complexity challenges (5 seconds: light off *kstest2* = 0.24, *P* = 0.0951 [n.s.]; light on *kstest2* = 0.26, *P* = 0.0560 [n.s.]; **Fig. 4B**, left top and bottom panels respectively; and 10 seconds: light off *kstest2* = 0.09, *P* = 0.7942 [n.s.]; **Fig. 4B**, right top panel). However, in the 10-second challenge with light stimulation, SNI-treated rats exhibited enhanced activity during the early period of the delay phase compared with controls (*kstest2* = 0.26, *P* = 0.0018; **Fig. 4B**, bottom right panel). In wrong trials (**Fig. 4C**), during the 5-second DNMS challenge, SNI-treated rats showed higher activity compared with controls (*kstest2* = 0.50, $P < 0.0001$; **Fig. 4C**, top left panel), which was annulled during light stimulation (*kstest2* = 0.08, *P* = 0.8871 [n.s.]; **Fig. 4C**, bottom left panel). During the 10-second challenge without stimulation,

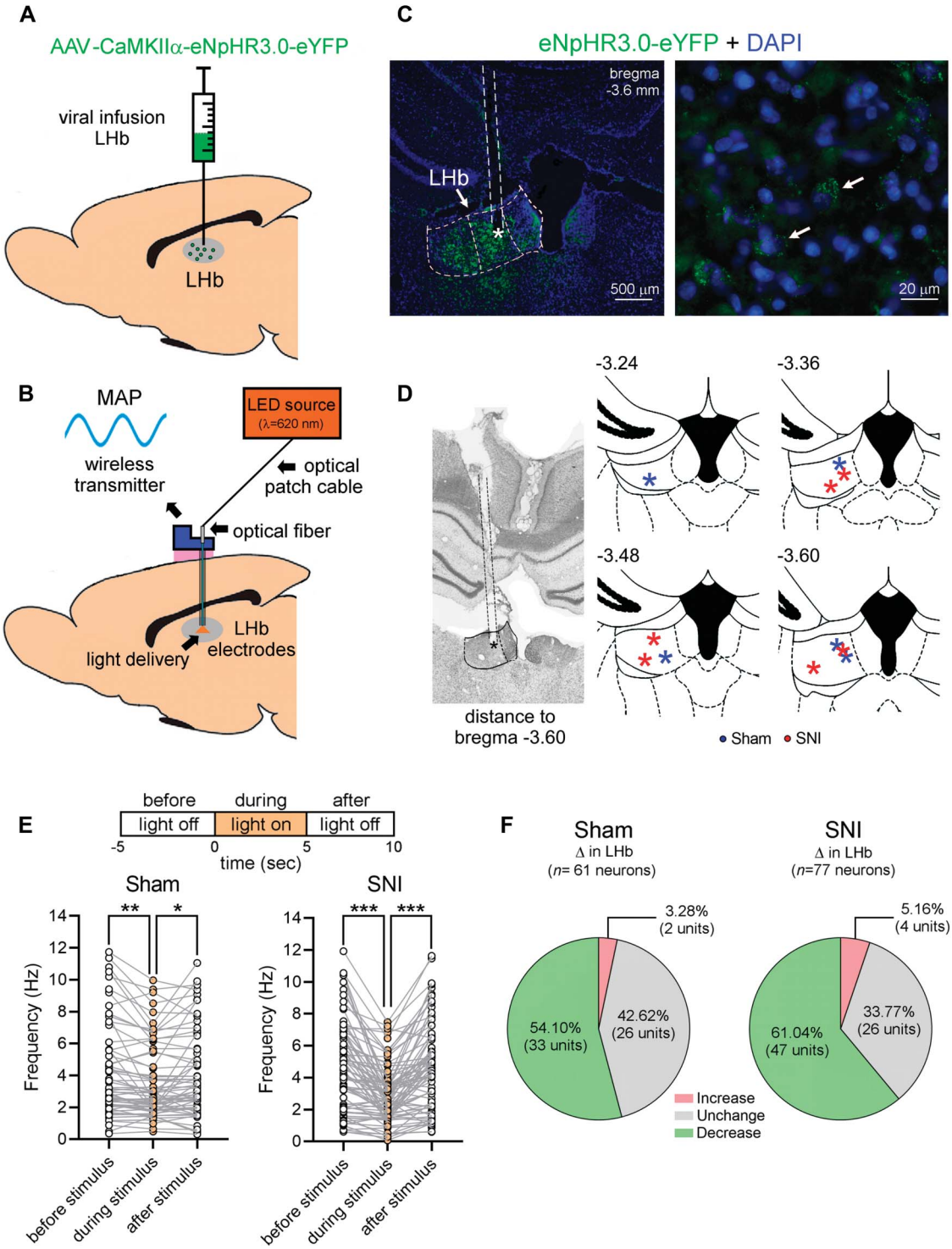

Figure 2. Expression of eNpHR3.0 opsin in LHb, light delivery and electrophysiological recording sites, and optogenetic light-dependent functional effects on LHb CaMKIIα-expressing excitatory neurons. (A) Strategy used to optogenetically inhibit LHb CaMKIIα-expressing neurons. AAV1-CaMKIIa-eNpHR3.0-eYFP viral particles were infused into the LHb. (B) Experimental setup used for light delivery and neural signals acquisition in the LHb. (C) The left panel shows a coronal illustration of green fluorescent protein (eYFP) labeling, which indicates the area of eNpHR3.0 transfection in the LHb. The right panel shows a magnified view of the LHb. Blue dots represent 4′,6-diamidino-2-phenylindole (DAPI) DNA-labeling used to nuclear counterstain. (D) Example of the optrode track (left panel; thionine-labeling microphotograph). The final location is indicated by a black asterisk, and the lesion track is marked by parallel black dotted lines. Coronal diagrams (right panels) illustrate the final positions of the optrode structure for sham (n = 5 rats, blue asterisks) and SNI rats (n = 6 rats, red asterisks). The upper number indicates the anterior-posterior distance to bregma. (E) Comparison of the mean firing activity before (5-second light-off, baseline), during (5-second light-on), and after the stimulus (5-second light-off) for each recorded neuron. Optogenetic stimulation using an orange LED light (continuous solid pulse at 5-6 mW @ 620 nm). (F) Percentage of recorded units with altered activity induced by light stimulation in the LHb for sham (left panel) and SNI (right panel) rats. Half of the units decreased their activity during optogenetic inhibition. Comparisons of firing activity between light stimulation phases were performed using a nonparametric Friedman test followed by a Dunn post hoc test. Experimental groups: sham, 61 units; SNI, 77 units. Significant results are indicated by * when $P < 0.05$, ** when $P < 0.01$, and *** when $P < 0.001$. LHb, lateral habenula; SNI, spared nerve injury.

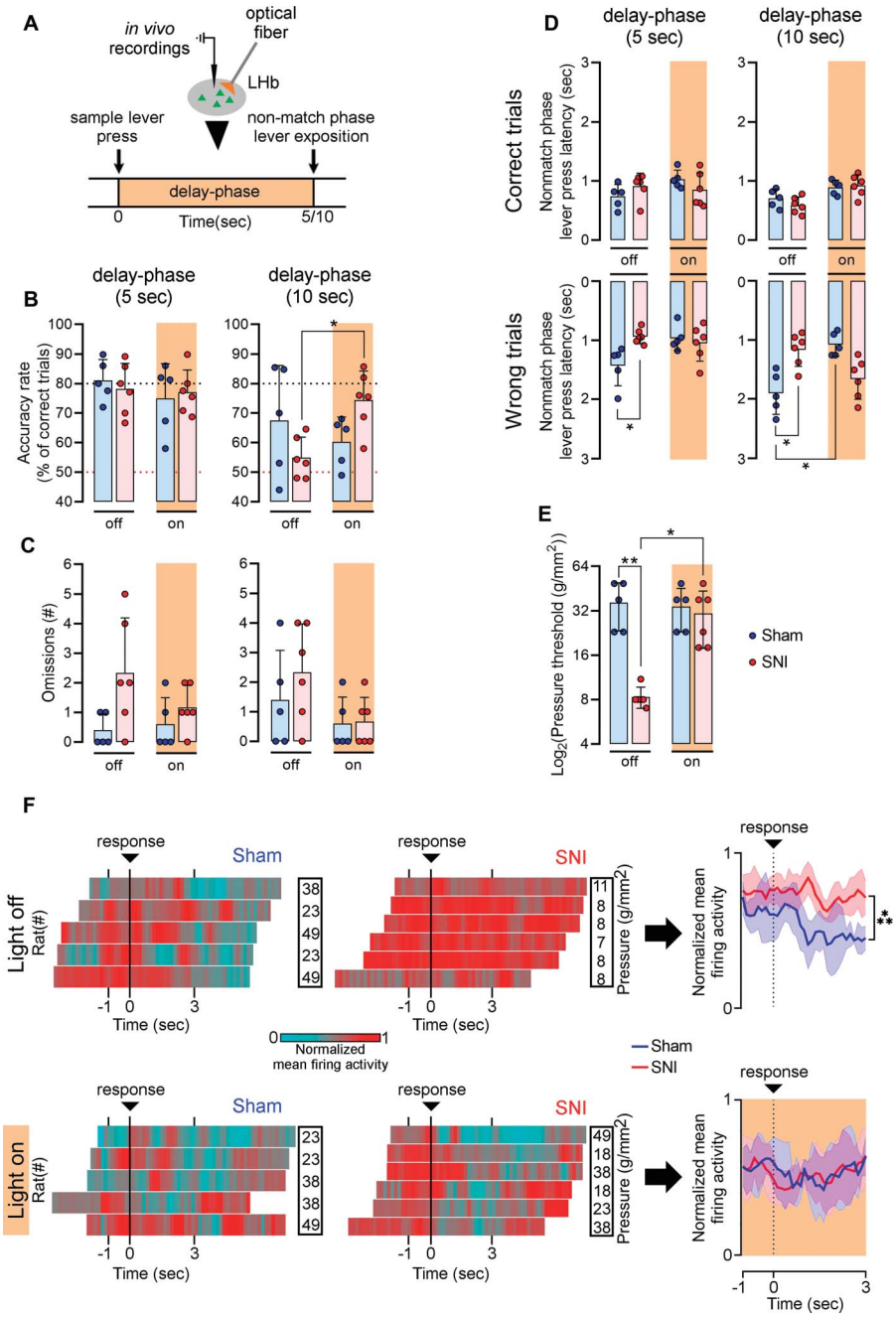

Figure 3. Optogenetic inhibition of LHb CaMKIIα-expressing neurons attenuates pain-related working memory deficits and peripheral pain responses. (A) Illustration of the experimental setup applied to selectivity neuromodulate LHb CaMKIIα-expressing neurons during the DNMS task delay phase. (B) DNMS task probe sessions accuracy rate (% of correct trials − rewarded trials) using a delay-phase challenge of 5 seconds (left panel) and 10 seconds (right panel). The inhibition of contralateral LHb of rats injected with AAV1-CaMKIIa-eNpHR3.0-eYFP induced an important recovery of SNI-treated rats' accuracy rate at the higher complexity challenges. (C) Mean number of omissions for all rats across 5-second (left panel) and 10-second (right panel) delay-phase challenges. Rats did not display significant differences in the number of omissions performed during behavioral contingencies. (D) Nonmatch phase lever press response latency related to correct trials and wrong trials. Rats did not display significant differences in their response latency profile during correct trials during behavioral contingencies. In turn, wrong trials were characterized by higher response latency values, particularly at the higher complexity challenge. (E) The level of mechanical sensitivity was measured 24 days after the lesion by withdrawal response to von Frey filaments stimulation. As expected, a large decrease was observed in the threshold required to induce a paw response in SNI-treated rats when compared with sham-treated rats without neuromodulation, which was reversed by inhibiting LHb-transfected neurons. (F) PETHs representing the normalized mean firing activity recorded in the LHb during the von Frey test (heatmaps, left panels). Each row corresponds to the averaged firing activity of a single recorded rat. Black vertical traces indicate the timing of the response evoked by the von Frey filament on the hindpaw. Vertical right values represent the pressure exerted by the von Frey filament as measured. The right panels display the normalized mean firing activity of all recorded rats per contingency. Firing distributions were compared using the activity within the time window around the response (−1, +3 seconds), and a 2-sample Kolmogorov-Smirnov test (*kstest2*, $P < 0.05$). Comparison between experimental groups and light protocols was performed using a nonparametric Kruskal-Wallis test followed by a Dunn post hoc test. Experimental groups: sham (n = 5 rats) and SNI (n = 6 rats). Significant results are indicated by * when $P < 0.05$, ** when $P < 0.01$, and *** when $P < 0.001$. Supplementary data regarding rats transfected with control virus AAV1-CaMKIIα-mCherry are provided in supplementary Fig. S4 (Appendix A, http://links.lww.com/PAIN/C184). DNMS, delayed nonmatch to sample; LHb, lateral habenula; PETH, perievent time histogram; SNI, spared nerve injury.

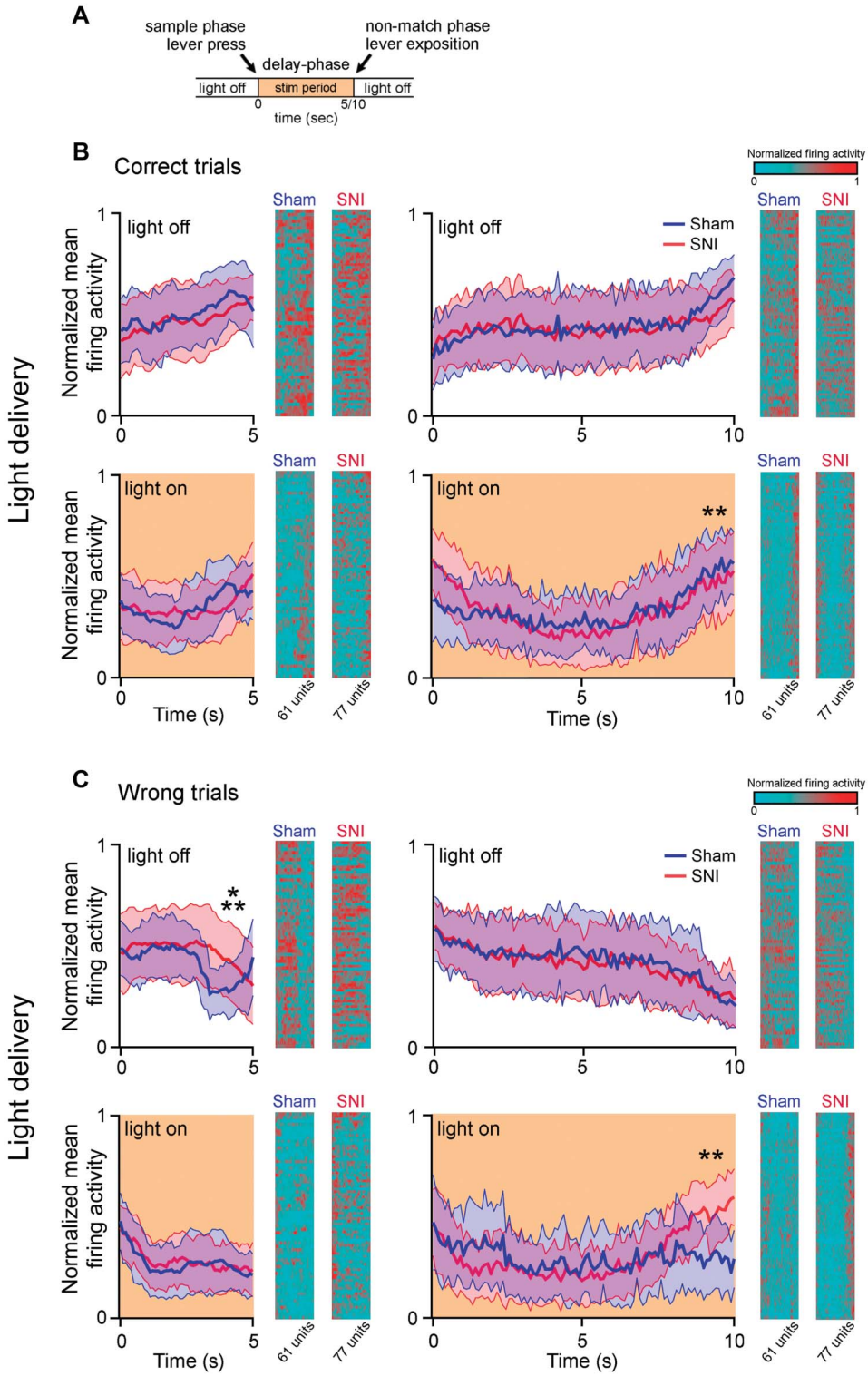

Figure 4. Effects of optogenetic light delivery in normalized LHb mean activity during the DNMS delay phase. (A) Illustration of the time window considered to compute the perievent time histograms (PETHs) during the DNMS delay phase. Normalized mean LHb activity during the DNMS delay phase (left panels), preceding correct (B) and wrong trials (C). Each experimental group exhibited distinct activity profiles under cognitive demand across the light delivery stimulation protocols. The most notable differences were observed during trials associated with wrong responses. Right heatmaps representing the task-related averaged activity of all recorded units with respect to behavioral contingency. Each row represents individual units (sham: n = 61 units; SNI: n = 77 units). Color code represents normalized firing activity (cyan, low; red, high activity). Comparison of populational mean firing distributions between experimental groups was performed using a 2-sample Kolmogorov-Smirnov test (*kstest2*, $P < 0.05$). Experimental groups: sham (n = 5 rats) and SNI (n = 6 rats). Significant results are indicated by ** when $P < 0.01$ and *** when $P < 0.001$. Data regarding sample lever press is provided in supplementary Fig. S1 (Appendix A, http://links.lww.com/PAIN/C184). DNMS, delayed nonmatch to sample; LHb, lateral habenula; SNI, spared nerve injury.

both groups showed similar activity (*kstest2* = 0.09, *P* = 0.7871 [n.s.]; **Fig. 4C**, top right panel). By contrast, with light stimulation, SNI-treated rats exhibited significantly enhanced activity towards the end of the delay phase (*kstest2* = 0.27, *P* = 0.0010; **Fig. 4C**, bottom right panel). Together, these data suggest that neuromodulation of LHb neurons may differently affect how these neurons process and integrate information critical for accurately selecting the correct lever, particularly during high-complexity challenges.

3.6. Lateral habenula neurons dynamically encode rewarded and nonrewarded trial information

To investigate the task-related activity of LHb-recorded neurons during DNMS task performance, we used PETHs to assess the firing signatures of neurons centered on the nonmatch phase lever press in both rewarded and nonrewarded trials. As shown in **Figure 5**, during correct trials (rewarded trials), most of the recorded units exhibited a decrease in firing activity following the lever press. **Figures 5B and C** illustrate an example of the activity of 2 LHb CaMKIIα-expressing neurons without or preceded by photoinhibition during the 5- and 10-second delay-phase challenge, respectively. In terms of the population neuronal firing distribution, for correct trials without photoinhibition, both experimental groups exhibited different activity distributions (5 seconds: *kstest2* = 0.53, *P* < 0.0001, **Fig. 5D**; and 10 seconds: *kstest2* = 0.40, *P* = 0.0022, **Fig. 5E**). During trials preceded by photoinhibition in the delay phase, no significant differences were observed under the 5-second challenge (*kstest2* = 0.25, *P* = 0.1393 [n.s.], **Fig. 5F**). However, for trials performed under the 10-second challenge, a different firing distribution was observed between experimental groups (*kstest2* = 0.40, *P* = 0.0021, **Fig. 5G**). In the case of wrong trials (nonrewarded trials) (**Fig. 6**), most recorded units displayed an increase in firing activity following the lever press. **Figures 6B and C** show an example of the activity of 2 neurons without and preceded by photoinhibition during the 5- and 10-second delay-phase challenge, respectively. Without photoinhibition during the 5-second delay-phase challenge, no significant differences were observed in the population firing activity distributions of both groups (*kstest2* = 0.28, *P* = 0.0796 [ns], **Fig. 6D**). For the 10-second delay-phase contingency, the increased activity of SNI recorded neurons was lower when compared with controls (*kstest2* = 0.48, *P* = 0.0002, **Fig. 6E**). In the case of wrong trials (nonrewarded trials) preceded by photoinhibition during the delay phase, we found significant differences between experimental groups (5 seconds: *kstest2* = 0.48, *P* = 0.0001, **Fig. 6F**; and 10 seconds: *kstest2* = 0.38, *P* = 0.0050, **Fig. 6G**). It is important to note that in the trials performed with a 10-second delay-phase challenge and preceded by photoinhibition of SNI neurons, the enhanced firing activity peak occurred just before the lever press. This suggests that the neuromodulation of LHb neurons may impact differently the way these neurons integrate information associated with the failure to obtain a reward, and it suggests a conscious anticipatory movement in encoding the response. We have also evaluated the changes in neuronal patterns during the sample phase lever exposure and the delay-phase time window. Supplementary Fig. S1 (Appendix A, http://links.lww.com/PAIN/C184) provides a complete view of these changes. In brief, our data showed that the sample phase was characterized by an enhanced LHb firing activity that preceded the lever exposure and by an activity depression after the press (supplementary Fig. S1a-d, http://links.lww.com/PAIN/C184).

3.7. The reorganization of intra-lateral habenula connectivity is associated with the encoding of nonrewarded trials in neuropathic pain rats

We investigated whether engagement in the task following optogenetic modulation leads to specific reorganization of intra-LHb activity in correct (rewarded trials) and wrong trials (nonrewarded trials) during the more complex 10-second trials. To assess whether the LHb-recorded neurons modulated their connectivity matrix according to the cognitive demand, we estimated the level of functional connectivity using PDC analysis.[5] **Figure 7** presents the quantification of bidirectional PDC levels between recorded neurons. For each trial, we used a time window of neuronal activity centered on the nonmatch phase lever press, taking into consideration the activity before and after the lever press (**Fig. 7A**).

In **Figure 7B**, we present an example of the LHb connectivity structure during correct trials (rewarded trials) for a sham and an SNI rat. The left panels display the activity of trials that were not preceded by optogenetic modulation during the delay phase, while the right panels display the activity preceded by neuromodulation. As shown, both rats did not exhibit a significant reorganization of their intra-LHb network during rewarded trials. For wrong trials (nonrewarded trials) (**Fig. 7C**), the sham rat did not exhibit a significant reorganization of the intra-LHb network during behavioral contingencies (**Fig. 7C**—top panels). However, the SNI rat showed strong intra-LHb connectivity during the trials that were not preceded by photoinhibition (**Fig. 7C**—left bottom panel). These patterns of activity were reduced during the trials preceded by photoinhibition (**Fig. 7C**—right bottom panel). A complete view of the intra-LHb network reorganization for all the rats included in this study is given in supplementary Figs. S2 and S3, http://links.lww.com/PAIN/C184. Concerning correct trials (**Fig. 7D**), no significant effect was observed for both experimental groups when comparing trials without or preceded by delay-phase neuromodulation. The statistical analyses showed a similar LHb neuronal connectivity organization for both experimental groups (sham-treated rats: Wilcoxon test [paired 2-tailed], light off vs on, *P* = 0.4137 [n.s.] [bidirectional pairs = 704], **Fig. 7D**—top panel; and SNI: light off vs on, *P* = 0.9034 [n.s.] [pairs = 952], **Fig. 7D**—bottom panel). Collectively, most neurons exhibited a residual paired PDC activity below 0.15. To further evaluate the impact of neuromodulation protocols on the segregation of connectivity strength of each bidirectional neuronal pair, we plotted the distribution of all neuronal cross-pairs per range of response. Both experimental groups showed similar distributions when comparing the stimulation contingencies in correct trials (sham-treated rats: light off vs on, *P* = 0.8125 [n.s.], **Fig. 7E**—top panel; and SNI: light off vs on, *P* = 0.9844 [n.s.], **Fig. 7E**—bottom panel). In the case of wrong trials, statistical analyses revealed that sham-treated rats did not show any differences between behavioral contingencies (light off vs on, *P* = 0.7355 [n.s.] [pairs = 704], **Fig. 7F**—top panel) and with a pattern similar to that obtained during correct trials. By contrast, SNI-treated rats revealed a significant decrease of their intra-LHb connectivity (light off vs on, *P* < 0.0001 [pairs = 952], **Fig. 7F**—bottom panel). The segregation of connectivity strength of each bidirectional neuronal pair per range of response showed no significant changes in sham-treated rats when comparing both behavioral contingencies (light off vs on, *P* = 0.8359, **Fig. 7G**—top panel). However, in the case of SNI-treated rats, the trials that were not preceded by delay-phase neuromodulation displayed a wider and stronger distribution of bidirectional paired activity compared with trials that were preceded by modulation. This resulted in

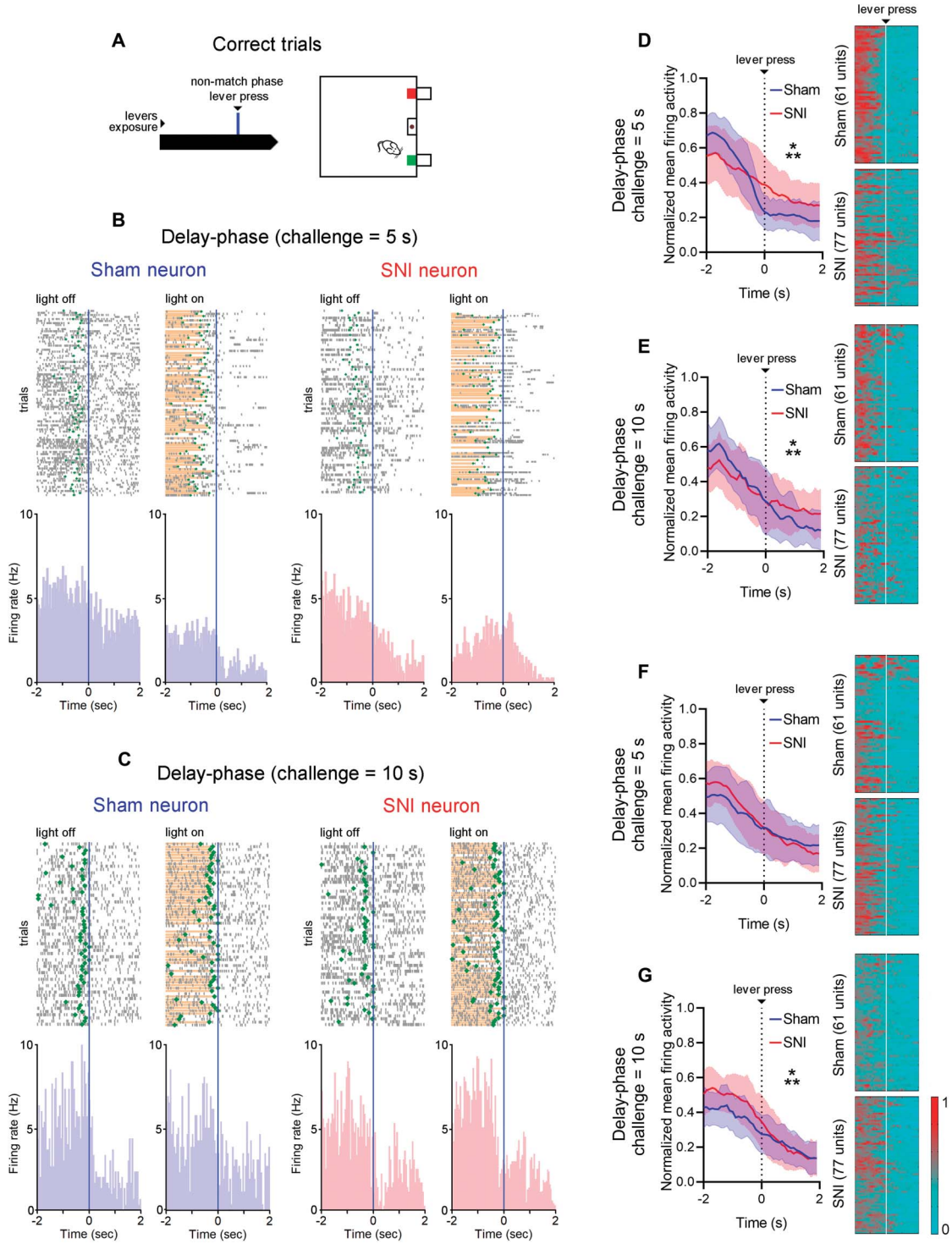

Figure 5. Correct trials were preceded by enhanced intra-LHb activity. (A) Illustration of the time window considered to compute the perievent time histograms (PETHs) during the nonmatch-to-sample lever press of correct rewarded trials. Example of PETHs of 2 LHb neurons recorded during (B) a 5-second and (C) a 10-second delay-phase challenge without and with optical neuromodulation. The trial sequence is shown in ascending order from bottom to top. The orange underline background indicates the period of optical stimulation that was captured, while green dots indicate lever exposure and the blue vertical line denotes the lever press. All neurons depicted exhibited enhanced activity that was depressed after the lever press. Normalized mean LHb activity during (D) 5-second and (E) 10-second delay-phase challenge trials conducted without prior optogenetic modulation. Normalized mean LHb activity traces during (F) 5-second and (G) 10-second delay-phase trials following prior optogenetic modulation. Right heatmaps representing the task-related activity of all recorded units with respect to behavioral contingency (sham: n = 61 units; SNI: n = 77 units). Each row represents individual units. Color code represents normalized firing activity (cyan, low; red, high activity). Comparison of populational mean firing distributions between experimental groups was performed using a 2-sample Kolmogorov-Smirnov test (*kstest2*, $P < 0.05$). Experimental groups: sham (n = 5 rats) and SNI (n = 6 rats). Significant results are indicated by *** when $P < 0.001$. LHb, lateral habenula; SNI, spared nerve injury.

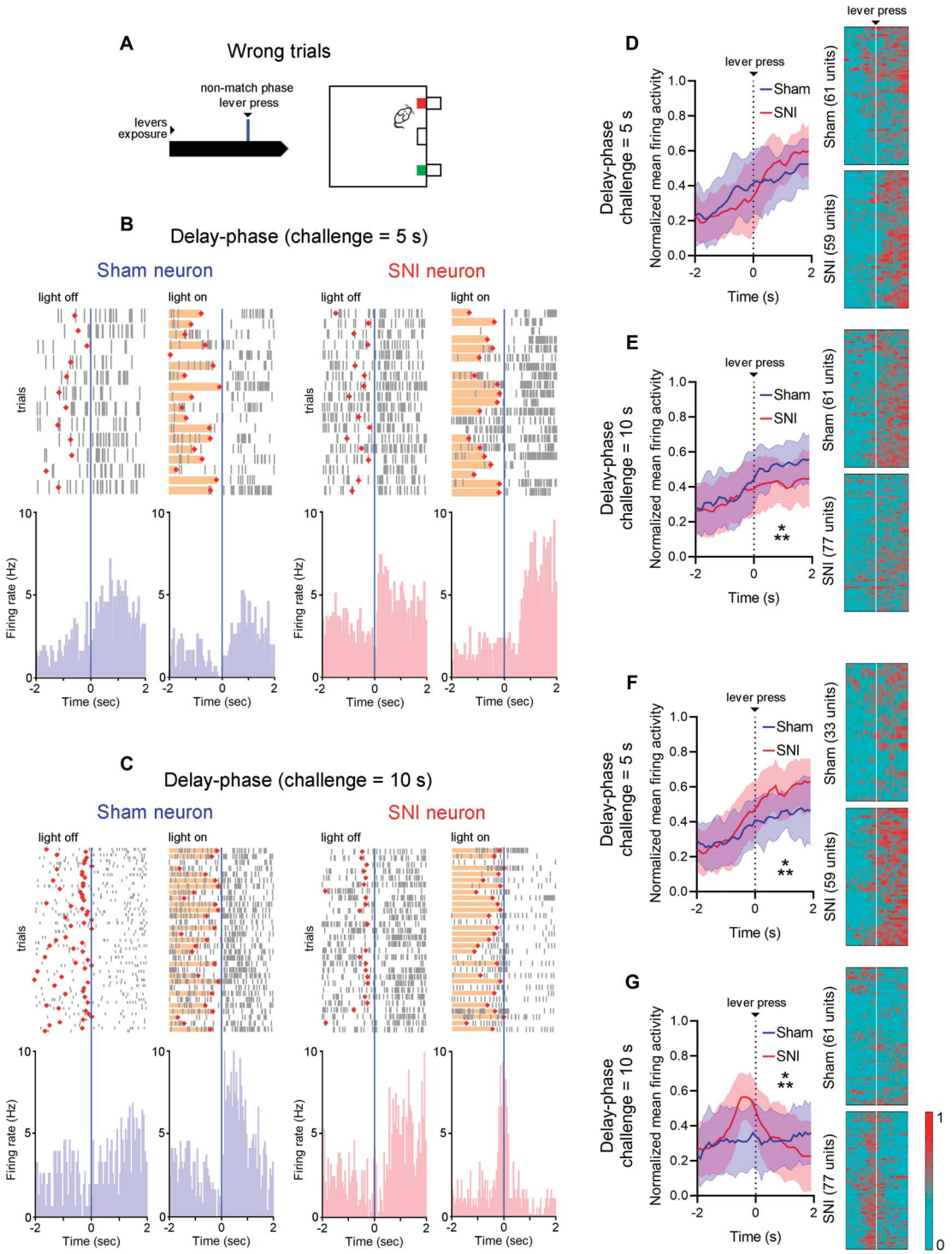

Figure 6. Wrong trials were accompanied by enhanced intra-LHb activity. (A) Illustration of the time window considered to compute the perievent time histograms (PETHs) during the nonmatch-to-sample lever press of wrong nonrewarded trials. Example of PETHs of 2 LHb neurons recorded during (B) a 5-second and (C) a 10-second delay-phase challenge without and with optical neuromodulation. The trial sequence is shown in ascending order from bottom to top. The orange underline background indicates the period of optical stimulation that was captured, while red dots indicate lever exposure and the blue vertical line denotes the lever press. All neurons depicted exhibited enhanced activity after the lever press. The exception was the SNI unit that revealed a peak of activity centered on the response during a 10-second delay-phase challenge. Normalized mean LHb activity during (D) 5-second and (E) 10-second delay-phase challenge trials conducted without prior optogenetic modulation. Normalized mean LHb activity traces during (F) 5-second and (G) 10-second delay-phase trials following prior optogenetic modulation. Right heatmaps representing the task-related activity of all recorded units with respect to behavioral contingency (sham: n = 61 units; SNI: n = 77 units). Each row represents individual units. Color code represents normalized firing activity (cyan, low; red, high activity). Comparison of populational mean firing distributions between experimental groups was performed using a 2-sample Kolmogorov-Smirnov test (*kstest2*, $P < 0.05$). Experimental groups: sham (n = 5 rats) and SNI (n = 6 rats). Significant results are indicated by *** when $P < 0.001$. LHb, lateral habenula; SNI, spared nerve injury.

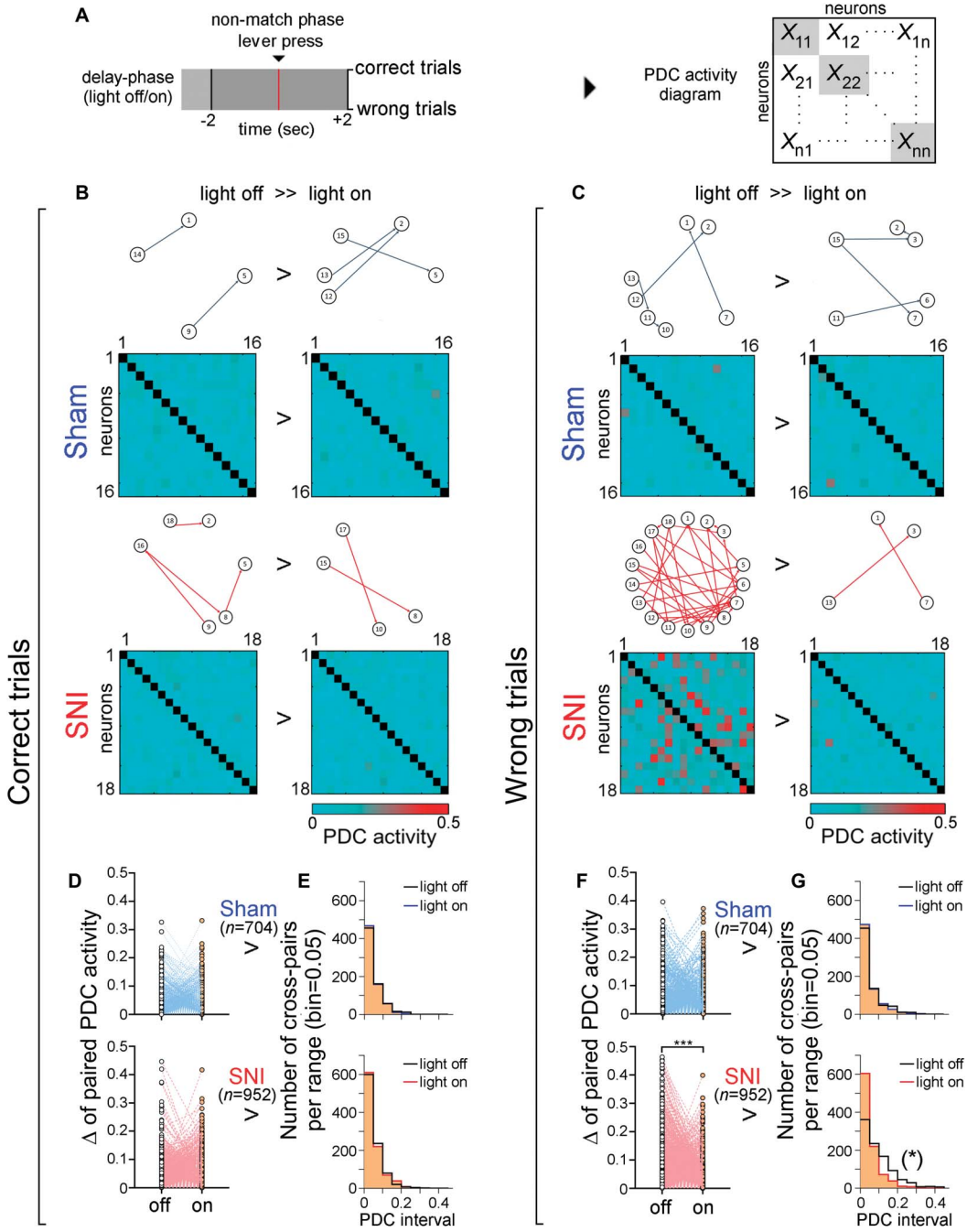

Figure 7. Neuropathic pain induced an intra-LHb connectome reorganization during higher complexity wrong nonrewarded trials. (A) Illustration of the time window used to characterize intra-LHb network connectivity (PDC) during rewarded and nonrewarded trials of a 10-second delay-phase challenge. Diagrams depicting the intra-LHb neural connectivity mutual influences associated with (B) correct and (C) wrong trials for a sham-treated rat and an SNI-treated rat (top panels). The threshold for significance is partial directed coherence (PDC) > 0.15. The correspondent output matrix for bidirectional paired intra-LHb neural PDC is shown in the bottom panels. The left panels represent the activity of trials not preceded by delay-phase LHb photoinhibition, while the right panels represent the activity of trials preceded by photoinhibition. The SNI-treated rat activity displayed enhanced intra-LHb connectivity during wrong (nonrewarded) trials not preceded by photoinhibition, which was not present in the group of trials performed with photoinhibition. (D) Comparison of PDC activity variation of each recorded neuronal pair during rewarded trials. No significant oscillations of paired PDC activity were observed during correct trials (top panel: sham group (n = 704); bottom panel: SNI group (n = 952)). (E) Distribution of PDC activity strength of each neuronal recorded pair per interval (bin resolution = 0.05) for sham-treated (top panels) and SNI-treated (bottom panels) rats. Both experimental groups displayed similar LHb PDC distributions. (F) Comparison of PDC activity variation of each recorded neuronal pair during wrong trials. SNI-treated rats (bottom panel) revealed a significant decrease in intra-LHb neural connectivity when wrong trials were preceded by delay-phase optogenetic photoinhibition. (G) Distribution of PDC activity strength of each neuronal recorded pair per interval for sham-treated (top panels) and SNI-treated (bottom panels) rats. SNI-treated rats during wrong trials not preceded by optogenetic photoinhibition displayed a wide range of connectivity (bottom left panel). Comparisons between light protocols were performed using a nonparametric Wilcoxon matched-pairs signed rank test (2-tailed, $P < 0.05$). Significant results are indicated by * when $P < 0.05$ and by *** when $P < 0.001$. Supplementary material is provided in Figs. S2 and S3 (Appendix A, http://links.lww.com/PAIN/C184). LHb, lateral habenula; SNI, spared nerve injury.

different regimes of local connectivity (light off vs on, $P = 0.0431$, **Fig. 7G**—bottom panel). These findings suggest that the intra-LHb network connectivity of SNI-treated rats plays an important role in encoding information related to the failure to obtain a reward.

4. Discussion

In this study, we have found that neuropathic pain-related WM memory impairments can be reversed by the optogenetic inhibition of LHb CaMKIIα-expressing neurons, resulting also in a significant reduction of pain responses. In addition, we observed that peripheral nerve injury alters the intra-LHb network activity related to reward information processing, particularly during nonrewarded trials. These findings expand our prior research that demonstrated the association between LHb-to-VTA glutamatergic signaling and the escalation of WM disturbances and structural changes in the VTA during inflammatory pain.[3]

It has been shown that chronic pain significantly reorganizes the LHb endogenous network.[22,44,49,70] Previous studies have shown that the LHb responds to noxious stimuli,[8,28] and imaging studies have reported bilateral activation of the habenular complex during noxious stimulation.[48,70] To inhibit pain responses, several methods have been used to restore intra-LHb balance,[26,47,69–71] suggesting the critical role of the LHb in pain processing. After 24 days of the peripheral lesion, we observed a greater reduction in pain threshold and higher intra-LHb spontaneous activity in SNI rats compared with the control group. In this study, we induced chronic neuropathic pain in rats using the protocol.[23] Our results demonstrated that contralateral inhibition of LHb CaMKIIα-expressing neurons can effectively reverse hyperalgesia in SNI-treated rats without sensitizing control rats, which is consistent with previous studies showing that activation of the habenula in neuropathic pain rats reduces their mechanical nociceptive threshold and increases depressive-like behaviors.[4,47] However, it is important to note that the direct inhibition of LHb glutamatergic neurons projecting into the VTA does not appear to have a strong impact on reducing peripheral inflammatory pain responses.[3] In part, this could be justified by the fact that the LHb exerts a modulatory drive over the VTA through indirect pathways with greater impact, such as through the rostromedial tegmental area,[34] or due to a differential impact of inflammatory and neuropathic pain in the LHb.[18,20,26] On the other hand, we also cannot overlook the fact that pain may induce structural changes in the VTA impacting pain processing directly.[33,73] In terms of the LHb, beta-CaMKII expression upregulation has also been linked to pain-associated depression comorbidity through the facilitation of glutamatergic synaptic transmission.[46,47] In addition, studies have shown that patients experiencing mood changes or pain exhibit increased habenular activity[59] and enhanced habenula-PFC and habenula-periaqueductal gray connectivity.[49,59] These findings support the idea that LHb plays a critical role in pain and mood regulation.

To investigate the role of the LHb in spatial memory encoding, we conducted a supplementary study using a classical spatial WM T-maze task[14] (refer to Appendix A—Fig. S5, http://links.lww.com/PAIN/C184 for details). Lateral habenula lesion was found to improve spatial memory accuracy in SNI-treated rats. These changes were not accompanied by any alteration in response latency or motor activity, indicating that pain does not change operant behavior following the lesion. In addition, decreased time in the central portion of the open field observed in SNI-treated rats without LHb lesion (classical anxiety–like behavior) was not a result of impaired motor activity (Appendix A—Fig. S5i, http://links.lww.com/PAIN/C184). These results align with previous studies showing that LHb lesions in hemiparkinsonian rats improved WM performance.[25] These data support the notion that LHb lesion does not prevent rats from being engaged in reward-seeking behavior. A comparable outcome was observed in rats with substantia nigra compacta lesions following intra-LHb activation of M-type potassium channels, resulting in decreased intra-LHb firing activity and increased dopamine (DA) and serotonin release in the ventromedial PFC.[9] In line with the results of LHb lesions, brief inhibition of LHb CaMKIIα-expressing neurons during the DNMS task delay phase also strongly enhanced WM performance in SNI-treated rats during higher complexity challenges. In contrast to the T-maze, we found significant changes in the response latency profile of control rats during wrong trials compared with SNI-treat rats. This suggests that control rats increased their impulsivity in the time window required to take a response. In this context, it has been reported that pharmacological inactivation of LHb can lead to an increase in perseverative errors during spatial a cue-switching task, indicating difficulty in adapting to learned rules.[7]

Disrupting LHb activity can impair the ability to differentiate reward delivery probabilities.[75] Because LHb neurons are inhibited by reward and excited by the absence of predicted rewards,[52,53] we examined their activity signatures during the performance of the DNMS task. The neural activity showed that most LHb neurons decreased their activity after a correct decision during rewarded trials while increasing their activity when an expected reward was omitted. An intriguing finding was the anticipatory LHb activity preceding wrong trials in SNI-treated rats, which was observed when optogenetic inhibition was applied during the delay phase. This is notable because LHb is believed to primarily contribute to reward-related processing by inhibiting VTA DA neurons.[52] The fact that this anticipatory activity resembles the heightened activity typically associated with rewarded responses suggests that, in SNI rats, optogenetic manipulation may artificially alter LHb activity, thereby reducing the expected inhibitory effect when a reward is not delivered. Another interesting finding was the behavioral specificity of LHb inhibition. Lateral habenula inhibition had no effect on persistence if rewards were not available, as evidenced by the lower number of wrong trials and omissions performed by SNI rats. In turn, activation of VTA GABA neurons has been associated with the disruption of reward consumption due to suppressed activity of neighboring DA neurons.[78] Lesioning the habenula formation in rodents has been linked to impaired reward processing, such as the inability to encode reward omission due to impaired downstream control of the DA neuron-modulated reward system.[76] This suggests that the inhibitory input from LHb plays a crucial role in determining reward-related activity in DA neurons. It has been proposed that these DA activations function as positive reward prediction errors (RPE), which in turn enhance reward predictions thought reinforcement learning.[36] This positive feedback loop between RPE and reward predictions perpetuates the pursuit of increasingly greater rewards. On the other hand, mechanisms that prevent DA inhibition reduce reward predictions, enabling smaller rewards to generate positive RPE signals, thus reinitiating the cycle towards the attainment of greater rewards.[19,27] In addition, LHb activity also responds to reward information that is unexpectedly cued or denied,[12] and this response appears to parallel the way in which DA neurons process positive RPE signals.

Despite the fact that LHb neurons do not have extensive axonal collaterals,[79] evidence suggests some degree of local

connectivity among these glutamatergic cells.[38] Our study found that the strength of intra-LHb neuronal connectivity precedes poor accuracy responses in pain rats during higher complexity challenges. These findings suggest that the intra-LHb network of SNI-treated rats plays an important role in encoding information related to the probability or failure to obtain rewards and supports the claim that LHb networks contribute to neuropathic pain-related cognitive impairments. Intra-connectivity within the LHb has been associated with modulating DA cell responses to aversive events.[13,77] Lateral habenula neurons are excited by aversive stimuli and associated predictive cues but are inhibited by rewarding cues.[53] While some LHb neurons indirectly inhibit reward-predicting DA cells,[35,74] other LHb projections directly excite DA cells within the VTA.[41] Optogenetic activation of this LHb-VTA pathway induces conditioned place avoidance, highlighting the crucial role that DA activation plays in aversive processing.[41] These findings suggest that the connectivity between the LHb and midbrain may be more related to saliency than the motivational valence of errors.

It is also important to note that the LHb exhibits connectivity with other areas that may influence its activity or output in reward salience encoding. For example, the medial PFC (mPFC) projects directly to the medial portion of the LHb[39,50] and is essential for relaying longitudinal information about environmental stimuli required to guide behavioral performance in tasks that demand high rates of sustained attention and engagement, such as spatial WM-dependent tasks. While the LHb does not send direct projections to mPFC, it likely interacts with it by modulating the activity of monoaminergic neurons that project to the mPFC.[41] In fact, rats trained in an operant delayed nonmatching to position task showed WM deficits following transient inactivation of the LHb, and bilateral disconnection of the mPFC-to-LHb pathway mimicked the effects of LHb silencing.[50] These findings suggest that changes in the activity of the mPFC or LHb can disrupt reward responses and behavioral flexibility, both of which are critical for goal-directed WM-dependent tasks. In this context, the LHb may play a key role in WM by signaling the absence of reward, thus shaping cognitive strategies in response to negative feedback.

In summary, this study provides new insights into how the intra-LHb network activity plays a key role in the stability and input selectivity necessary to guide behavior responses for cognitive flexibility control. These findings suggest that restoring the balance of intra-LHb connectivity may be an important target for reversing cognitive deficits during neuropathic pain conditions. However, a study limitation is the potential influence of sex-specific effects on the LHb, given the well-documented sex-based differences in pain processing, including in LHb-dependent functions. Future research could clarify how these differences impact neuropathic pain phenotypes.

Conflict of interest statement

The authors declare that they have no known competing financial interests or personal relationships that could have appeared to influence the work reported in this article.

Acknowledgements

This work was funded by National Funds through Fundação para a Ciência e Tecnologia—FCT Project 2022.05193.PTDC—doi: 10.54499/2022.05193. PTDC (V.G.). Additional support was obtained by Operational Competitiveness (POCI) Program—COMPETE2020 and National Funds through FCT Project PTDC/MED-NEU/28181/2017 (H.C.-C.) and FCT Project PTDC/MED-NEU/28498/2017 (V.G.)); FCT Individual Employment Contract 2022.00128.CEECind—doi: 10.54499/2022.00128.CEECIND/CP1735/CT0019 and DL 57/2016/CP1355/CT0015—doi: 10.54499/DL57/2016/CP1355/CT0015 (H. C.-C), and FCT PhD-grant SFRH/BD/70522/2010 (M.D.).

Data availability: The datasets used or analyzed during this study are available from the corresponding author upon reasonable request.

Author's contributions. C.M. and H.C.-C. designed research; C.M. and H.C.-C. performed research, H.C.-C. and V.G. analyzed data; C.M., H.C.-C., and V.G. wrote the article.

Supplemental digital content

Supplemental digital content associated with this article can be found online at http://links.lww.com/PAIN/C185 and http://links.lww.com/PAIN/C184.

Article history:
Received 7 June 2024
Received in revised form 25 October 2024
Accepted 26 October 2024
Available online ■■■

References

[1] Aguiar P, Mendonca L, Galhardo V. OpenControl: a free opensource software for video tracking and automated control of behavioral mazes. J Neurosci Methods 2007;166:66–72.
[2] Aizawa H, Yanagihara S, Kobayashi M, Niisato K, Takekawa T, Harukuni R, McHugh TJ, Fukai T, Isomura Y, Okamoto H. The synchronous activity of lateral habenular neurons is essential for regulating hippocampal theta oscillation. J Neurosci 2013;33:8909–21.
[3] Alemi M, Pereira AR, Cerqueira-Nunes M, Monteiro C, Galhardo V, Cardoso-Cruz H. Role of glutamatergic projections from lateral habenula to ventral tegmental area in inflammatory pain-related spatial working memory deficits. Biomedicines 2023;11:820.
[4] Antunes GF, Pinheiro Campos AC, de Assis DV, Gouveia FV, de Jesus Seno MD, Pagano RL, Ruiz Martinez RC. Habenula activation patterns in a preclinical model of neuropathic pain accompanied by depressive-like behaviour. PLoS One 2022;17:e0271295.
[5] Baccalá LA, Sameshima K. Partial directed coherence: a new concept in neural structure determination. Biol Cybern 2001;84:463–74.
[6] Baker PM, Jhou T, Li B, Matsumoto M, Mizumori SJ, Stephenson-Jones M, Vicentic A. The lateral habenula circuitry: reward processing and cognitive control. J Neurosci 2016;36:11482–8.
[7] Baker PM, Raynor SA, Francis NT, Mizumori SJ. Lateral habenula integration of proactive and retroactive information mediates behavioral flexibility. Neuroscience 2017;345:89–98.
[8] Benabid AL, Jeaugey L. Cells of the rat lateral habenula respond to high-threshold somatosensory inputs. Neurosci Lett 1989;96:289–94.
[9] Bian G, Liu J, Guo Y, Yang Y, Li L, Qiao H, Li W, Xu T, Zhang Q. Kv7.2 subunit-containing M-type potassium channels in the lateral habenula are involved in the regulation of working memory in parkinsonian rats. Neuropharmacology 2020;168:108012.
[10] Bianco IH, Wilson SW. The habenular nuclei: a conserved asymmetric relay station in the vertebrate brain. Philos Trans R Soc Lond B Biol Sci 2009;364:1005–20.
[11] Boulos LJ, Darcq E, Kieffer BL. Translating the habenula-from rodents to humans. Biol Psychiatry 2017;81:296–305.
[12] Bromberg-Martin ES, Matsumoto M, Hikosaka O. Dopamine in motivational control: rewarding, aversive, and alerting. Neuron 2010;68:815–34.
[13] Brown PL, Palacorolla H, Brady D, Riegger K, Elmer GI, Shepard PD. Habenula-induced inhibition of midbrain dopamine neurons is diminished by lesions of the rostromedial tegmental nucleus. J Neurosci 2017;37:217–25.
[14] Cardoso-Cruz H, Dourado M, Monteiro C, Galhardo V. Blockade of dopamine D2 receptors disrupts intrahippocampal connectivity and enhances pain-related working memory deficits in neuropathic pain rats. Eur J Pain 2018;22:1002–15.
[15] Cardoso-Cruz H, Lima D, Galhardo V. Instability of spatial encoding by CA1 hippocampal place cells after peripheral nerve injury. Eur J Neurosci 2011;33:2255–64.

[16] Cardoso-Cruz H, Paiva P, Monteiro C, Galhardo V. Selective optogenetic inhibition of medial prefrontal glutamatergic neurons reverses working memory deficits induced by neuropathic pain. PAIN 2019;160:805–23.
[17] Cerqueira-Nunes M, Monteiro C, Galhardo V, Cardoso-Cruz H. Orbitostriatal encoding of reward delayed gratification and impulsivity in chronic pain. Brain Res 2024;1839:149044.
[18] Cohen SR, Melzack R. The habenula and pain: repeated electrical stimulation produces prolonged analgesia but lesions have no effect on formalin pain or morphine analgesia. Behav Brain Res 1993;54:171–8.
[19] Creed MC, Ntamati NR, Tan KR. VTA GABA neurons modulate specific learning behaviors through the control of dopamine and cholinergic systems. Front Behav Neurosci 2014;8:8.
[20] Cui WQ, Zhang WW, Chen T, Li Q, Xu F, Mao-Ying QL, Mi WL, Wang YQ, Chu YX. Tacr3 in the lateral habenula differentially regulates orofacial allodynia and anxiety-like behaviors in a mouse model of trigeminal neuralgia. Acta Neuropathol Commun 2020;8:44.
[21] Curtis CE, D'Esposito M. Persistent activity in the prefrontal cortex during working memory. Trends Cogn Sci 2003;7:415–23.
[22] Dai D, Li W, Chen A, Gao XF, Xiong L. Lateral habenula and its potential roles in pain and related behaviors. ACS Chem Neurosci 2022;13:1108–18.
[23] Decosterd I, Woolf CJ. Spared nerve injury: an animal model of persistent peripheral neuropathic pain. PAIN 2000;87:149–58.
[24] Dick BD, Rashiq S. Disruption of attention and working memory traces in individuals with chronic pain. Anesth Analg 2007;104:1223–9. tables of contents.
[25] Du CX, Liu J, Guo Y, Zhang L, Zhang QJ. Lesions of the lateral habenula improve working memory performance in hemiparkinsonian rats. Neurosci Lett 2018;662:162–6.
[26] Du Y, Wu YX, Guo F, Qu FH, Hu TT, Tan B, Wang Y, Hu WW, Chen Z, Zhang SH. Lateral habenula serves as a potential therapeutic target for neuropathic pain. Neurosci Bull 2021;37:1339–44.
[27] Flores-Dourojeanni JP, van den Munkhof MH, Luijendijk MCM, Vanderschuren L, Adan RAH. Inhibition of ventral tegmental area projections to the nucleus accumbens shell increases premature responding in the five-choice serial reaction time task in rats. Brain Struct Funct 2023;228:787–98.
[28] Gao DM, Hoffman D, Benabid AL. Simultaneous recording of spontaneous activities and nociceptive responses from neurons in the pars compacta of substantia nigra and in the lateral habenula. Eur J Neurosci 1996;8:1474–8.
[29] Goshen I, Brodsky M, Prakash R, Wallace J, Gradinaru V, Ramakrishnan C, Deisseroth K. Dynamics of retrieval strategies for remote memories. Cell 2011;147:678–89.
[30] Goutagny R, Loureiro M, Jackson J, Chaumont J, Williams S, Isope P, Kelche C, Cassel JC, Lecourtier L. Interactions between the lateral habenula and the hippocampus: implication for spatial memory processes. Neuropsychopharmacol 2013;38:2418–26.
[31] Guo Y, Zhang L, Zhang J, Du CX, Lv SX, Wang T, Wang HS, Xie W, Liu J. Activation and blockade of serotonin(4) receptors in the lateral habenula improve working memory in unilateral 6-hydroxydopamine-lesioned Parkinson's rats. Neurol Res 2019;41:585–93.
[32] Han S, Wang J, Zhang W, Tian X. Chronic pain-related cognitive deficits: preclinical insights into molecular, cellular, and circuit mechanisms. Mol Neurobiol 2024;61:8123–43.
[33] Huang S, Borgland SL, Zamponi GW. Peripheral nerve injury-induced alterations in VTA neuron firing properties. Mol Brain 2019;12:89.
[34] Jhou TC, Fields HL, Baxter MG, Saper CB, Holland PC. The rostromedial tegmental nucleus (RMTg), a GABAergic afferent to midbrain dopamine neurons, encodes aversive stimuli and inhibits motor responses. Neuron 2009;61:786–800.
[35] Ji H, Shepard PD. Lateral habenula stimulation inhibits rat midbrain dopamine neurons through a GABA(A) receptor-mediated mechanism. J Neurosci 2007;27:6923–30.
[36] Keiflin R, Pribut HJ, Shah NB, Janak PH. Ventral tegmental dopamine neurons participate in reward identity predictions. Curr Biol 2019;29:93–103.e3.
[37] Kim M, Mawla I, Albrecht DS, Admon R, Torrado-Carvajal A, Bergan C, Protsenko E, Kumar P, Edwards RR, Saha A, Napadow V, Pizzagalli DA, Loggia ML. Striatal hypofunction as a neural correlate of mood alterations in chronic pain patients. Neuroimage 2020;211:116656.
[38] Kim U, Chang SY. Dendritic morphology, local circuitry, and intrinsic electrophysiology of neurons in the rat medial and lateral habenular nuclei of the epithalamus. J Comp Neurol 2005;483:236–50.
[39] Kim U, Lee T. Topography of descending projections from anterior insular and medial prefrontal regions to the lateral habenula of the epithalamus in the rat. Eur J Neurosci 2012;35:1253–69.
[40] King SG, Gaudreault PO, Malaker P, Kim JW, Alia-Klein N, Xu J, Goldstein RZ. Prefrontal-habenular microstructural impairments in human cocaine and heroin addiction. Neuron 2022;110:3820–32.e4.
[41] Lammel S, Lim BK, Ran C, Huang KW, Betley MJ, Tye KM, Deisseroth K, Malenka RC. Input-specific control of reward and aversion in the ventral tegmental area. Nature 2012;491:212–7.
[42] Lecourtier L, Neijt HC, Kelly PH. Habenula lesions cause impaired cognitive performance in rats: implications for schizophrenia. Eur J Neurosci 2004;19:2551–60.
[43] Leite-Almeida H, Cerqueira JJ, Wei H, Ribeiro-Costa N, Anjos-Martins H, Sousa N, Pertovaara A, Almeida A. Differential effects of left/right neuropathy on rats' anxiety and cognitive behavior. PAIN 2012;153:2218–25.
[44] Li J, Li Y, Zhang B, Shen X, Zhao H. Why depression and pain often coexist and mutually reinforce: role of the lateral habenula. Exp Neurol 2016;284:106–13.
[45] Li J, Yang S, Liu X, Han Y, Li Y, Feng J, Zhao H. Hypoactivity of the lateral habenula contributes to negative symptoms and cognitive dysfunction of schizophrenia in rats. Exp Neurol 2019;318:165–73.
[46] Li K, Zhou T, Liao L, Yang Z, Wong C, Henn F, Malinow R, Yates JR III, Hu H. βCaMKII in lateral habenula mediates core symptoms of depression. Science 2013;341:1016–20.
[47] Li Y, Wang Y, Xuan C, Li Y, Piao L, Li J, Zhao H. Role of the lateral habenula in pain-associated depression. Front Behav Neurosci 2017;11:31.
[48] Manssuer L, Ding Q, Zhang Y, Gong H, Liu W, Yang R, Zhang C, Zhao Y, Pan Y, Zhan S, Li D, Sun B, Voon V. Risk and aversion coding in human habenula high gamma activity. Brain 2022;146:2642–53.
[49] Mao CP, Chen FR, Huo JH, Zhang L, Zhang GR, Zhang B, Zhou XQ. Altered resting-state functional connectivity and effective connectivity of the habenula in irritable bowel syndrome: a cross-sectional and machine learning study. Hum Brain Mapp 2020;41:3655–66.
[50] Mathis V, Barbelivien A, Majchrzak M, Mathis C, Cassel JC, Lecourtier L. The lateral habenula as a relay of cortical information to process working memory. Cereb Cortex 2017;27:5485–95.
[51] Mathis V, Cosquer B, Avallone M, Cassel JC, Lecourtier L. Excitatory transmission to the lateral habenula is critical for encoding and retrieval of spatial memory. Neuropsychopharmacol 2015;40:2843–51.
[52] Matsumoto M, Hikosaka O. Lateral habenula as a source of negative reward signals in dopamine neurons. Nature 2007;447:1111–5.
[53] Matsumoto M, Hikosaka O. Representation of negative motivational value in the primate lateral habenula. Nat Neurosci 2009;12:77–84.
[54] Mazza S, Frot M, Rey AE. A comprehensive literature review of chronic pain and memory. Prog Neuropsychopharmacol Biol Psychiatry 2018;87:183–92.
[55] Mizumori SJY, Baker PM. The lateral habenula and adaptive behaviors. Trends Neurosci 2017;40:481–93.
[56] Mondoloni S, Mameli M, Congiu M. Reward and aversion encoding in the lateral habenula for innate and learned behaviours. Transl Psychiatry 2022;12:3.
[57] Monteiro C, Cardoso-Cruz H, Matos M, Dourado M, Lima D, Galhardo V. Increased fronto-hippocampal connectivity in the Prrxl1 knockout mouse model of congenital hypoalgesia. PAIN 2016;157:2045–56.
[58] Moriarty O, McGuire BE, Finn DP. The effect of pain on cognitive function: a review of clinical and preclinical research. Prog Neurobiol 2011;93:385–404.
[59] Morris JS, Smith KA, Cowen PJ, Friston KJ, Dolan RJ. Covariation of activity in habenula and dorsal raphe nuclei following tryptophan depletion. Neuroimage 1999;10:163–72.
[60] Paxinos G, Watson C. The rat brain in stereotaxic coordinates. San Diego: Academic, 1998.
[61] Pereira AR, Alemi M, Cerqueira-Nunes M, Monteiro C, Galhardo V, Cardoso-Cruz H. Dynamics of lateral habenula-ventral tegmental area microcircuit on pain-related cognitive dysfunctions. Neurol Int 2023;15:1303–19.
[62] Proulx CD, Aronson S, Milivojevic D, Molina C, Loi A, Monk B, Shabel SJ, Malinow R. A neural pathway controlling motivation to exert effort. Proc Natl Acad Sci U S A 2018;115:5792–7.
[63] Riley MR, Constantinidis C. Role of prefrontal persistent activity in working memory. Front Syst Neurosci 2015;9:181.
[64] Sacher J, Neumann J, Funfstuck T, Soliman A, Villringer A, Schroeter ML. Mapping the depressed brain: a meta-analysis of structural and functional alterations in major depressive disorder. J Affect Disord 2012;140:142–8.
[65] Sanders D, Simkiss D, Braddy D, Baccus S, Morton T, Cannady R, Weaver N, Rose JE, Levin ED. Nicotinic receptors in the habenula: importance for memory. Neuroscience 2010;166:386–90.
[66] Sartorius A, Kiening KL, Kirsch P, von Gall CC, Haberkorn U, Unterberg AW, Henn FA, Meyer-Lindenberg A. Remission of major depression

under deep brain stimulation of the lateral habenula in a therapy-refractory patient. Biol Psychiatry 2010;67:e9–11.
[67] Seminowicz DA, Davis KD. Cortical responses to pain in healthy individuals depends on pain catastrophizing. PAIN 2006;120:297–306.
[68] Seo J, Kim SH, Kim YT, Song HJ, Lee JJ, Kim SH, Han SW, Nam EJ, Kim SK, Lee HJ, Lee SJ, Chang Y. Working memory impairment in fibromyalgia patients associated with altered frontoparietal memory network. PLoS One 2012;7:e37808.
[69] Shelton L, Becerra L, Borsook D. Unmasking the mysteries of the habenula in pain and analgesia. Prog Neurobiol 2012;96:208–19.
[70] Shelton L, Pendse G, Maleki N, Moulton EA, Lebel A, Becerra L, Borsook D. Mapping pain activation and connectivity of the human habenula. J Neurophysiol 2012;107:2633–48.
[71] Shen X, Ruan X, Zhao H. Stimulation of midbrain dopaminergic structures modifies firing rates of rat lateral habenula neurons. PLoS One 2012;7: e34323.
[72] Shumake J, Ilango A, Scheich H, Wetzel W, Ohl FW. Differential neuromodulation of acquisition and retrieval of avoidance learning by the lateral habenula and ventral tegmental area. J Neurosci 2010;30: 5876–83.
[73] Sotres-Bayón F, Torres-López E, López-Avila A, del Angel R, Pellicer F. Lesion and electrical stimulation of the ventral tegmental area modify persistent nociceptive behavior in the rat. Brain Res 2001;898:342–9.
[74] Stamatakis AM, Stuber GD. Optogenetic strategies to dissect the neural circuits that underlie reward and addiction. Cold Spring Harb Perspect Med 2012;2:a011924.
[75] Stopper CM, Floresco SB. What's better for me? Fundamental role for lateral habenula in promoting subjective decision biases. Nat Neurosci 2014;17:33–5.
[76] Tian J, Uchida N. Habenula lesions reveal that multiple mechanisms underlie dopamine prediction errors. Neuron 2015;87:1304–16.
[77] Trusel M, Nuno-Perez A, Lecca S, Harada H, Lalive AL, Congiu M, Takemoto K, Takahashi T, Ferraguti F, Mameli M. Punishment-predictive cues guide avoidance through potentiation of hypothalamus-to-habenula synapses. Neuron 2019;102:120–7.e4.
[78] van Zessen R, Phillips JL, Budygin EA, Stuber GD. Activation of VTA GABA neurons disrupts reward consumption. Neuron 2012;73:1184–94.
[79] Weiss T, Veh RW. Morphological and electrophysiological characteristics of neurons within identified subnuclei of the lateral habenula in rat brain slices. Neuroscience 2011;172:74–93.
[80] Yang LM, Hu B, Xia YH, Zhang BL, Zhao H. Lateral habenula lesions improve the behavioral response in depressed rats via increasing the serotonin level in dorsal raphe nucleus. Behav Brain Res 2008;188: 84–90.
[81] Zimmermann M Ethical guidelines for investigations of experimental pain in conscious animals. PAIN 1983;16:109–10.